Article

Novel and Integrated Process for the Valorization of Kraft Lignin to Produce Lignin-Containing Vitrimers

Ajinkya More, Thomas Elder, Nicolò Pajer, Dimitris S. Argyropoulos, and Zhihua Jiang*

Read Online

ACCESS | Metrics & More | Article Recommendations | Supporting Information

ABSTRACT: The valorization of lignin into value-added products by oxidative conversion is a widely studied strategy. However, in many cases, this approach has limited scope for integration into industrial processes. The objective of our work is to maximize overall lignin utilization to produce diverse value-added products with a focus on integration in the existing industrial pulp and paper processes. The utilization of the sequential oxidation strategy using oxygen and ozone resulted in kraft lignin with a marked improvement in carboxyl content and also allowed the formation of vanillin and vanillic acid in the oxygen stage. The sequentially oxidized lignin (OxL-COOH) was then cured with poly(ethylene glycol) diglycidyl ether (PEG-epoxy) to form high-lignin-content (>48 wt %) vitrimers with high thermal stability, fast relaxation, swelling, and self-healing due to the presence of bond-exchangeable cross-linked networks. Overall, this study provides a novel approach for the multidimensional valorization of lignin and demonstrates an integrated approach for kraft lignin valorization in the pulp and paper industry.
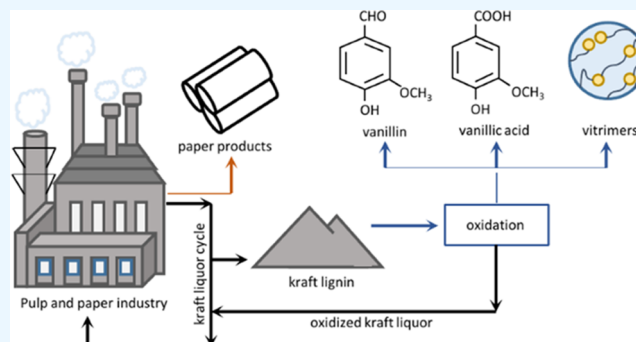
INTRODUCTION

Currently, the disposal of thermoset waste in our environment is one of the most challenging problems that needs to be addressed. Due to the lack of suitable methods for recycling or repair, most of the thermoset waste is disposed of by incineration and landfill.[1] The concept of circular economy, which was introduced by the Ellen MacArthur Foundation, allows for a sustainable future for generations to come.[2] Two key aspects of this concept involve that the vast majority of thermoset waste should be reusable and that the materials used in the chain should be bio-based. Conventional epoxy-based thermosets possess excellent hardness, adhesion, and chemical resistance; however, once damaged, they cannot be repaired by heating due to the presence of a permanently cross-linked network. To address this issue, researchers have considered the modification of thermosetting polymers using vitrimer chemistry.[3−6] This allows for the introduction of dynamic covalent linkages in the cross-linked network, which imparts repairability and recyclability to thermosetting polymers. However, the recently developed vitrimer materials are based on petrochemical feedstocks. Therefore, the utilization of bio-based renewable feedstocks in the vitrimer matrix is crucial to fit into the concept of a circular economy.[7−9]

Lignin is one such bio-based renewable feedstock that is abundantly available and accounts for about 30% of nonfossil carbon on earth.[10−12] The lignin obtained from technical processes has different structural properties and characteristics based on how the delignification is accomplished, the recovery process, and wood species.[13,14] Kraft lignin accounts for about 85% of all lignin produced worldwide, which corresponds to ~45 million metric tons per year. It is mainly utilized as a source of low-grade fuel in the pulping operation, and only about 100 000 tons of it is valorized every year.[15,16] Oxidative conversion of lignin to produce vanillin (4-hydroxy-3-methoxy benzaldehyde, $C_8H_8O_3$) and vanillic acid (4-hydroxy-3-methoxy benzoic acid, $C_8H_8O_4$) is widely proposed.[17−20] Vanillin is one of the most widely produced aromatic aldehydes worldwide. It has useful applications in the food, cosmetic, chemical, and pharmaceutical industries.[21,22] Recently, vanillic acid has also been gaining interest due to its antibacterial, antimicrobial, and chemopreventive properties.[23] Oxidative conversion of kraft lignin using oxygen is preferred due to its environmental friendliness, high atom economy, and low price. Current approaches of oxidative conversion of lignin using oxygen apply the oxygen oxidation treatment as an additional and standalone step to kraft lignin after its isolation from black liquor.
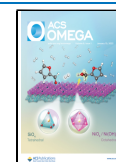
Scheme 1. (a) LignoForce Process and (b) Modified LignoForce Process for the Development of High-Value Products[27] (Reproduced in Part with Permission from the American Chemical Society)
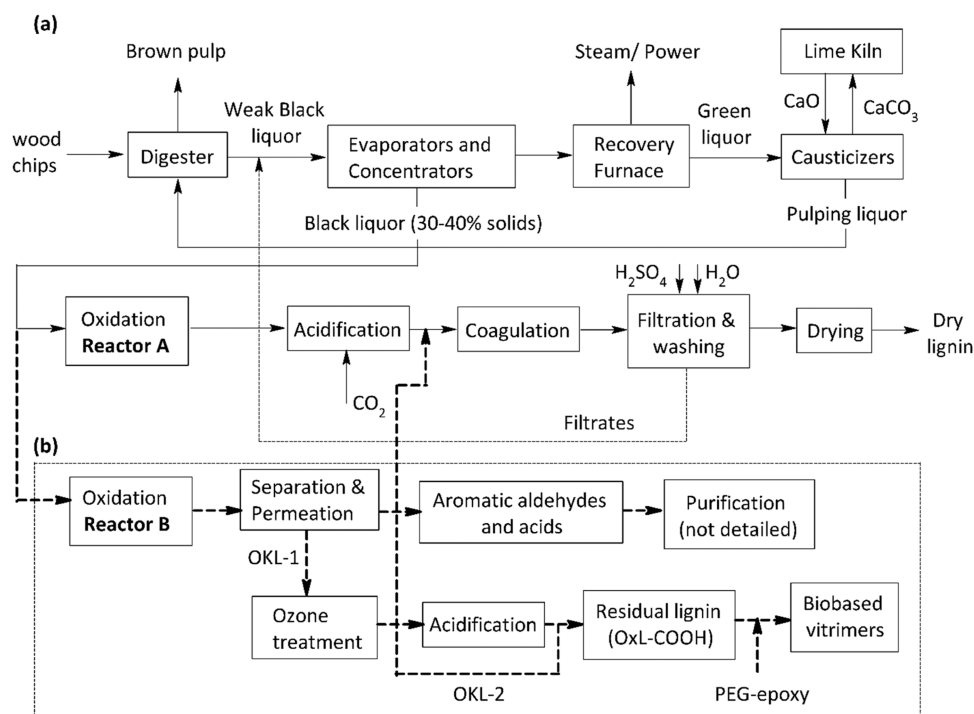
Scheme 2. Proposed Reaction Pathway for Vitrimer Formation[a]

Note - 'R' denotes lignin
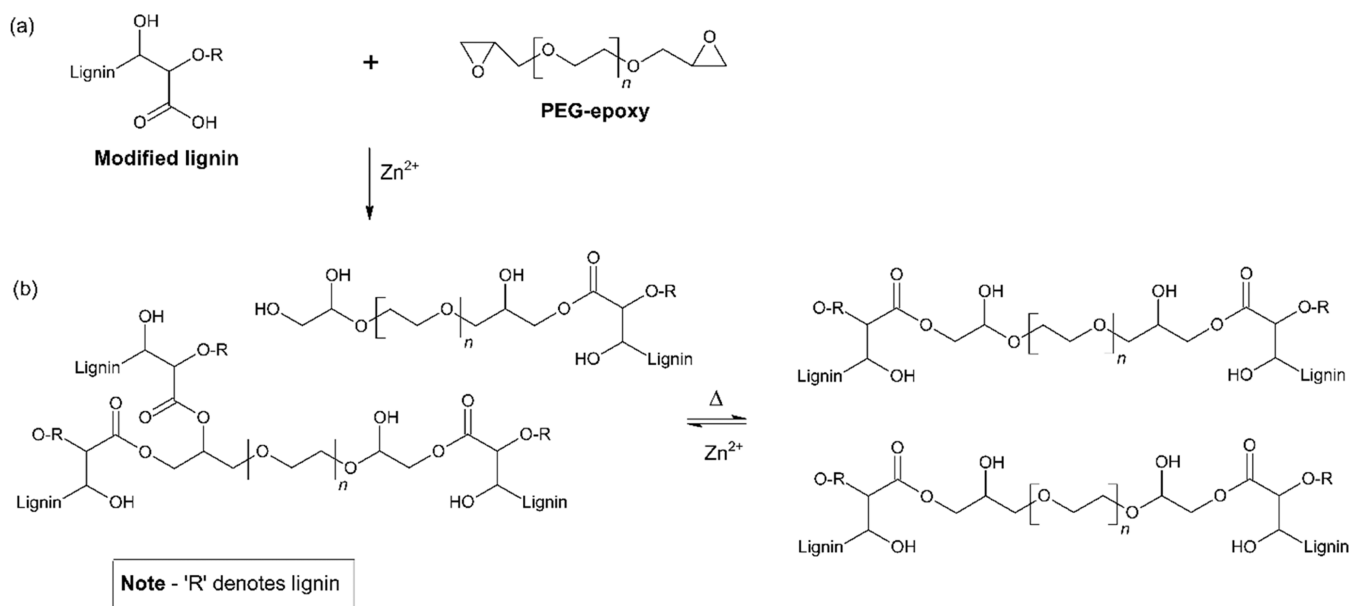
[a](a) Curing reaction of OxL-COOH and PEG-epoxy and (b) transesterification exchange reaction (TER) within the cross-linked network.

Recently, the addition of an oxygen stage in the lignin recovery cycle from black liquor has been gaining interest.[24−26] Scheme 1a shows the LignoForce process jointly developed by FPInnovations and NORAM.[27] In this novel process, an oxygen oxidation step is incorporated into the lignin recovery process for improving the overall efficiency of the lignin recovery process and reducing the emission of volatile sulfur and organic compounds. Building on the LignoForce process, we proposed a novel and integrated process for the valorization of kraft lignin (Scheme 1b). In this

proposed process, the oxygen oxidation step was optimized for producing vanillin and vanillic acid. The optimization of oxygen oxidation to form vanillin and vanillic acid was reported in our previous paper.[28] In this work, we studied the effect of oxygen and ozone oxidation of kraft lignin to understand the functional group changes under the LignoForce operating conditions. The oxygen oxidation was then followed by ozone treatment to induce a significant amount of carboxyl groups. The kraft liquor obtained after oxygen oxidation is termed "OKL-1" and the liquor obtained after ozone oxidation is

termed "OKL-2." After the ozone treatment, the modified lignin (OxL-COOH) is then precipitated by acidification. Further, OxL-COOH, which is a rich source of carboxyl groups, is cured with poly(ethylene glycol) diglycidyl ether (PEG-epoxy) to form lignin-containing vitrimers.

Among the various vitrimer formation chemistries reported in the literature, transesterification is most suitable for oxidized kraft lignin conversion into vitrimers.[5,29,30] New studies based on vitrimer polymers also use enzymatic hydrolysis lignin, which can be modified by epoxidation and direct carboxylation strategies.[31,32] In this study, sequential oxidation for kraft lignin was used as a tool to form vanillin and vanillic acid products from oxygen oxidation followed by ozone oxidation for carboxyl content improvement in kraft lignin. As shown in Scheme 2a, the modified lignin is a result of sequential oxidation using oxygen and ozone (OxL-COOH). During oxidation, electrophilic attack at lignin centers of high electron density can cause the formation of a four-membered cyclic peroxide intermediate, which tends to rearrange and induce cleavage of carbon−carbon bonds.[33−36]

In the first step, the modified lignin (OxL-COOH) reacts with PEG-epoxy to cause ring opening to produce an ester bond and a secondary hydroxyl group. This secondary hydroxyl group can further react with the −COOH group to form an ester. In Scheme 2b, bond rearrangement takes place without a disruption in connectivity due to reversible exchange reactions.[37] The stoichiometric ratio "R", which relates to the ratio of epoxy to carboxyl groups, can be varied to form different curing systems. In principle, the "R" value is correlated to the amount of lignin present in the vitrimers. The objective of this work is to maximize the overall lignin utilization to produce lignin-containing vitrimers with a focus on integration in the existing pulp and paper industrial processes.

■ EXPERIMENTAL SECTION

Materials. Oxygen and nitrogen of ultrahigh purity were supplied by Airgas USA (purity ≥97%); sulfuric acid (1.0 N laboratory reagent grade) and ethanol (200 proof) were purchased from VWR chemicals; poly(ethylene glycol) diglycidyl ether (PEG-epoxy, Sigma-Aldrich, M_n = 500 g mol^{-1}), $Zn(acac)_2$ (Sigma-Aldrich, 99.995%), and sodium chloride (assay ≥99%) were supplied by Fischer Chemical. Sodium hydroxide beads (purity ≥97%) and hydrochloric acid (1.0 N laboratory reagent grade) were purchased from VWR Chemicals.

Oxidation of Softwood Kraft Lignin (SKL). *Oxygen Oxidation of SKL.* Oxygen oxidation was performed according to the literature.[28] Oxidation experiments were carried out in a Parr reactor with a capacity of 1 L (Series 4520). The heating and temperature were controlled with a Parr 4848 reactor controller. Temperature and total pressure inside the reactor were measured using a Type J (iron-constantan) thermocouple and a pressure gauge, respectively. The agitator speed was kept constant at 400 rpm for all runs. In total, 20 g of lignin was dissolved in 200 mL of an alkaline solution containing 26.67 g of NaOH. After complete dissolution, the resulting mixture was diluted to a final volume of 333 mL. This concentration of lignin (20 g in 333 mL of solution) was kept constant for all experiments performed. The resulting solution was introduced into the reactor and initially pressurized to 30 psi using nitrogen. The reactor was then heated until the temperature set point was reached. After the temperature set point was reached, oxygen was introduced to the reactor and the reaction time was monitored from the point of admission of oxygen. The reactor was pressurized with 50 psi of oxygen for all experiments according to the literature. The effect of temperature on the yield of vanillin and vanillic acid and the carboxyl content of lignin was studied at 120, 130, 140, 150, and 160 °C at a constant reaction time of 40 min.

The operating conditions described above were maintained constant for the experiments performed at temperatures (T_i) of 80, 88, and 96 °C to understand the functional group content changes under the LignoForce operating conditions, which was studied using ^{31}P NMR.

Ozone Oxidation and Sequential Oxidation Using Oxygen and Ozone. Ozone is a highly reactive oxidizing agent capable of oxidizing most types of lignin structures. Therefore, oxidation of oxygen-pretreated lignin with ozone will result in a further increase in the carboxyl content. The ozonation treatment was carried out at ambient pressure in a glass bubbler with a capacity of 1 L. The details of the ozonation procedure are described in the literature.[38] The glass bubbler was heated to 80 °C in a water bath with constant stirring. A flow of ozone was supplied by a "5G Lab Benchtop Ozone Generator" from A2Z Ozone providing an ozone dosage of 5000 mg h^{-1} (100% capacity, oxygen flow rate 2 LPM). The ozone was directly injected into the solution through a long capillary. The off-gas was vented through a wash bottle partially filled with a 10% by weight potassium iodide solution. Ozonation was carried out at different time intervals of 1, 2, 3, and 4 h to optimize the carboxyl content in the modified lignin. The optimized conditions for oxygen and ozone oxidations were then used to sequentially oxidize kraft liquor obtained after oxygen oxidation (OKL-1) at 130 °C for 40 min followed by ozone oxidation at 80 °C for 2 h.

Preparation of OxL-COOH/PEG-Epoxy Vitrimers. The formulation of OxL-COOH/PEG-epoxy systems was varied based on the stoichiometric ratio "R", which represents the ratio of epoxy groups to carboxyl groups. For R:1, 1.5 g of lignin (OxL-COOH) was allowed to dissolve in 200 proof ethanol (1:3 w/v). After it was dissolved, 1.53 g of PEG-epoxy was added followed by 80.3 mg of $Zn(acac)_2$ (5 mol % based on carbonyl content in OxL-COOH). For R:1.3, 1.5 g of lignin (OxL-COOH) was allowed to dissolve in 200 proof ethanol (1:3 w/v). After it was dissolved, 1.98 g of PEG-epoxy was added followed by 80.3 mg of $Zn(acac)_2$ (5 mol % based on carbonyl content in OxL-COOH). For R:1.5, 1.5 g of lignin (OxL-COOH) was allowed to dissolve in 200 proof ethanol (1:3 w/v). After it was dissolved, 2.29 g of PEG-epoxy was added followed by 80.3 mg of $Zn(acac)_2$ (5 mol % based on carbonyl content in OxL-COOH). The use of ethanol as a solvent allows the mixing of all of the components before curing the reaction. Softwood kraft lignin is hydrophobic and apolar solvents are unable to dissolve the lignin. Also, the introduction of −COOH groups in OxL-COOH results in added affinity toward polar solvents. Aliphatic alcohols have varying abilities to dissolve lignin due to the different numbers of carbon atoms present in them. A higher number of carbon atoms in the aliphatic alcohol are prone to have less mobility and more steric hindrance to surround the lignin moieties. Therefore, ethanol, which has a limited number of carbon atoms and reasonable polarity, represents a suitable solvent to homogenize all of the components in the solution. All of the components were homogeneous in the solvent system, which is a key parameter for uniform vitrimer film formation. The

optimized solvent evaporation experiments were conducted by heating at 25 °C for 1 h followed by heating for 1, 2, 3, and 4 h at 80, 90, 100, and 110 °C, respectively. The optimum conditions for uniform film formation were observed at 110 °C with a heating duration of 4 h. After solvent evaporation, the homogeneous solution was cured in a PTFE mold at 150 °C for 1 h and postcured at 190 °C for 2 h.

Characterization of the Lignin and Lignin-Containing Vitrimers. *^{31}P NMR Spectroscopy.* Samples were characterized using *N*-hydroxy-5-norbornene-2,3-dicarboxylic acid imide (NHND) as an internal standard according to the literature.[39] Before performing the hydroxyl group determination, samples were dried in a vacuum chamber set at 40 °C overnight. Briefly, 30 mg of the accurately weighted sample was mixed with 500 μL of a pyridine/deuterochloroform mixture (1.6/1 v/v), 100 μL of the internal standard solution (NHND in pyridine/deuterochloroform + chromium(III) acetylacetonate as a relaxation agent) and stirred to dissolve the lignin. In the case of the untreated SKL sample, degraded, five drops of *N,N′*-dimethyl formamide were added to the mixture to favor its dissolution. Then, the sample was derivatized by the addition of 100 μL of 1-choro-4,4′,5,5′-tetramethyl-1,3,2-dioxaphospholane. The spectra of the phosphorous-labeled lignin preparations were recorded using a 500 MHz Bruker Nuclear Magnetic Resonance Spectrometer. The acquisition parameters used are reported in Table 1, and the spectra have been integrated and processed using MestReNova software, as shown in Figure S1.

Table 1. Acquisition Parameters for ^{31}P NMR

Parameter	Description
pulse program	inverse gated decoupling pulse (zgig)
nucleus	^{31}P
spectral width	100 ppm
acquisition time	0.8 s
relaxation delay	10 s
number of scans	128
center of spectrum	140 ppm

Conductometric Titration. The carboxyl contents of the oxygen-treated lignin (L-COOH), ozone-treated lignin (OzL-COOH), and sequentially oxidized lignin (OxL-COOH) were determined using the conductometric titration method described in the literature.[40] After the oxidation treatment, a sample of lignin solution was adjusted to pH below 2 by the addition of HCl. As a result, the lignin is precipitated from the solution and recovered by centrifugation followed by freeze-drying. In general, 1.5 g of the freeze-dried lignin sample (with moisture content ≤10% by weight) was added to 300 mL of 0.10 N HCl and stirred for 1 h. The lignin was then filtered and washed with deionized water to ensure that the conductivity of effluent water was less than 5 μS cm^{-1}. Further, the washed lignin was dispersed in 0.001 N NaCl (250 mL), followed by the addition of a 0.10 N HCl solution (1.5 mL). The resultant dispersion was stirred and titrated with 0.05 N NaOH under continuous bubbling of nitrogen. The conductometric titration was performed using a Metrohm Autotitrator equipped with an 856 Conductivity Module connected to the main module (888 Titrando) coupled with Tiamo 2.5 software. The output plot of conductivity against the volume of NaOH results in a parabolic curve with three distinguishable regimes. The first regime is the decrease in

conductivity associated with the neutralization of added HCl. The second regime is usually a horizontal zone that corresponds to the neutralization of weak acid groups, i.e., carboxylic acid groups. Finally, the third regime is linked to the increase in conductivity after reaching the equivalence point due to the introduction of excess NaOH to the suspension.

Fourier Transform Infrared Spectroscopy. FTIR measurements were performed using a Thermo Scientific Nicolet 6700 FTIR instrument equipped with attenuated total reflection (ATR). Each spectrum was collected with 64 scans in the wavenumber range of 4000−400 cm^{-1} at a resolution of 4 cm^{-1}. Background spectra were recorded before every sample. The spectra were analyzed using OMNIC 7.3 software.

Dynamic Mechanical Analysis. The storage modulus of all films was characterized with dynamic mechanical analysis (DMA, Dynamic Mechanical Analyzer TA Instruments RSA III) in a tensile mode at a 1% min^{-1} strain rate. The dimensions of the test specimen were ~30 mm × 10 mm × 0.4 mm. Samples were scanned from −40 to 150 °C at a heating rate of 5 °C min^{-1}. The frequency and the amplitude were set at 1 Hz and 15 μm, respectively.

Stress Relaxation Test. Isothermal stress relaxation tests were performed with an 8 mm parallel plate geometry. The thickness of the sample was ~0.4 mm. An axial force of 2 N was applied to attain good contact of the sample with the parallel plate. During the test, 1% strain was applied and the trend of modulus as a function of time was recorded.

Thermogravimetric Analysis. The thermal stability of the samples was examined using a TA Instruments Q-50 thermogravimetric analysis (TGA) system. The sample was loaded into a platinum pan and scanned from 25 to 800 °C at a heating rate of 10 °C min^{-1} under a nitrogen atmosphere.

Self-Healing. The thermal repair of the films was studied by monitoring the recovery of scratches by an OLYMPUS 52 ×7 optical microscope. A crack was made on the surface of the film using a razor blade, and the width of the crack was determined using the microscope (d_1). The cracked film was placed in between two tin plates and clamped using clips to fix the tin plates. This system was then placed in a convection oven at 200 °C for heating durations from 0 to 30 min, and the sample was observed every 15 min. The width change of the crack was measured using the microscope (d_2), and the rate of repair was calculated using eq 1.

$$R = \frac{d_2 - d_1}{d_1} \times 100\% \tag{1}$$

Swelling Study. The swelling of the OxL-COOH/PEG-epoxy system was determined in aqueous NaOH solutions at room temperature. In general, the swelling ratio can be based on weight or volume changes in the sample. In this work, the swelling ratio was defined based on the weight changes in the sample. The sample with dimensions of 0.5 cm × 0.5 cm × 0.1 cm was weighed (W_1) and added to a 20 mL glass vial containing aqueous NaOH solutions with concentrations of 0.01, 0.05, 0.1, and 0.2 M (10 mL) for 10 min. The glass vial was capped and kept still at room temperature. At time intervals of 5, 10, 15, 20, 30, and 60 min, the sample was taken out, the free water was wiped off with a filter paper, and the sample weight was measured (W_2). The percentage swelling (S_r) at a given time was calculated according to eq 2.
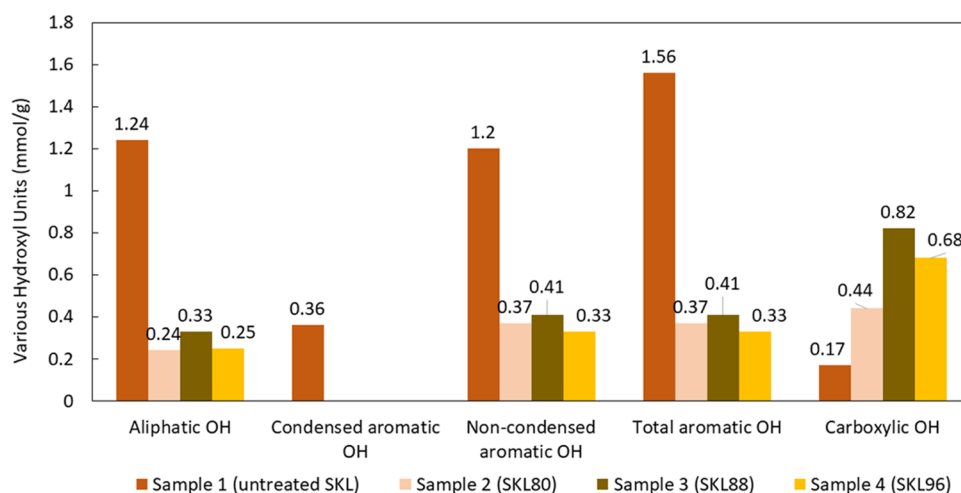
Figure 1. Changes in various hydroxyl units present in softwood kraft lignin before and after oxidation using ^{31}P NMR.

$$S_r = \frac{W_2 - W_1}{W_1} \times 100\%$$

(2)

RESULTS AND DISCUSSION

Sequential Oxidation of Softwood Kraft Lignin. The oxygen oxidation of softwood kraft lignin was performed at 80, 88, and 96 °C to study the changes in functional group content. Among the known reactions that occur in lignin during oxidation is the formation of a significant amount of carboxylic OH units that facilitate subsequent dissolution. This is evidenced by the gradual increase of the carboxylic OH content of the untreated SKL from 0.17 to 0.82 mmol g^{-1} for sample 3 treated at 88 °C, as shown in Figure 1. The formation of carboxylic acid groups is accompanied by the elimination of aliphatic hydroxyl groups. The aliphatic OH units in untreated SKL reduced from 1.24 to 0.24 mmol g^{-1} for sample 2 treated at 80 °C. Similar results after oxygen oxidation treatment were also reported in the literature.[41,42]

Ozone is a highly reactive oxidizing agent capable of reacting with all types of lignin structures.[43] Since the carboxylic OH units show progressive formation among the various hydroxyl units investigated, the structural changes obtained from ozone are focused on the changes in carboxylic OH units under similar operating conditions. Also, complete degradation of the aromatic ring in lignin occurs if ozonation is conducted at high pressures and if ozone is present in excess; therefore, in the present study, the ozone treatment was performed at ambient pressure. The variation of severity with respect to reaction duration is shown in Figures S2 and 2, graphically representing the changes in the amount of carboxylic OH units versus the time duration of ozonation. The error bars in Figure 2 signify the standard deviation of the carboxyl content obtained at a given time duration. As the severity of ozone treatment increases, the amount of carboxylic OH units formed gradually increases reaching a plateau region in the ozonation time duration from 2 to 3 h. Beyond this region, a slight decrease in the carboxyl content is observed with increasing duration of the reaction. It is possible that the consumption of available ozone by radical species limits the lignin degradation in this region.

In our previous work, we also demonstrated the effect of oxygen oxidation on carboxyl content in softwood kraft lignin (SKL).[28] The optimum carboxyl content of 1.41 mmol g^{-1} was
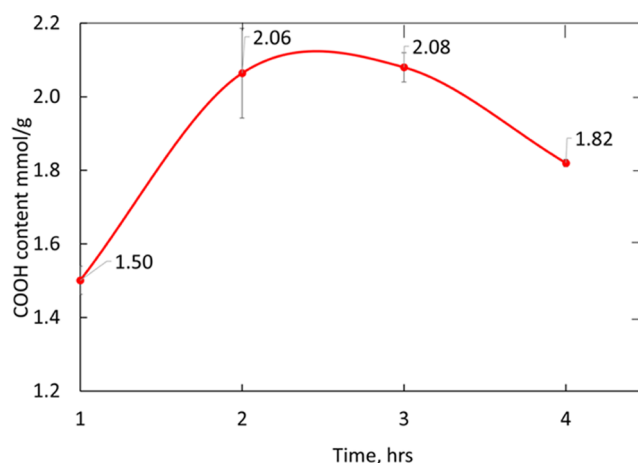
Figure 2. Changes in carboxylic OH groups in SKL after ozone oxidation using conductometric titration (the bars on the values indicate standard deviation).

obtained in the modified lignin (L-COOH) using oxygen at 130 °C for 40 min of reaction time. Therefore, for an integrated process, the softwood kraft lignin utilized under these conditions is beneficial, as it also allows the formation of vanillin and vanillic acid, which are high-value products. The oxidized kraft liquor (OKL-1) obtained at these conditions from oxygen oxidation was then further treated with ozone at 80 °C for 2 h to analyze the formation of carboxylic OH units due to their progressive formation during oxidation under different conditions. It was observed that the sequentially oxidized softwood kraft lignin (OxL-COOH) had a carboxylic OH unit content of 4.06 mmol g^{-1} (Figure S3), which is significantly higher than that in the isolated treatment of oxygen and ozone. The presence of carboxyl groups in lignin is known to improve solubilization in polar solvents and vitrimer formation.[33,44−46]

Film Formation. Vitrimers exhibit superior strength and repairability properties due to the dynamic transesterification reaction in a cross-linked network. However, one of the key phenomena that also allows vitrimers to possess these properties is the "film formation" during the curing process. For the first time, in our work, we discuss the main factors that govern the uniform and nonporous film formation in vitrimers, which is only briefly discussed in the recent literature.[47−50]
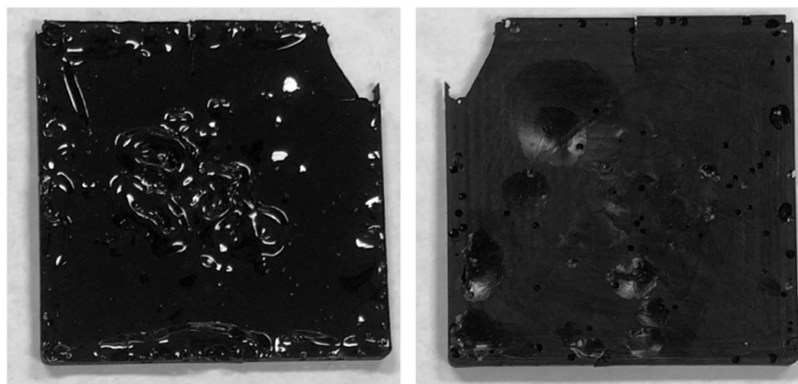
Figure 3. Bubble formation in vitrimers before troubleshooting.
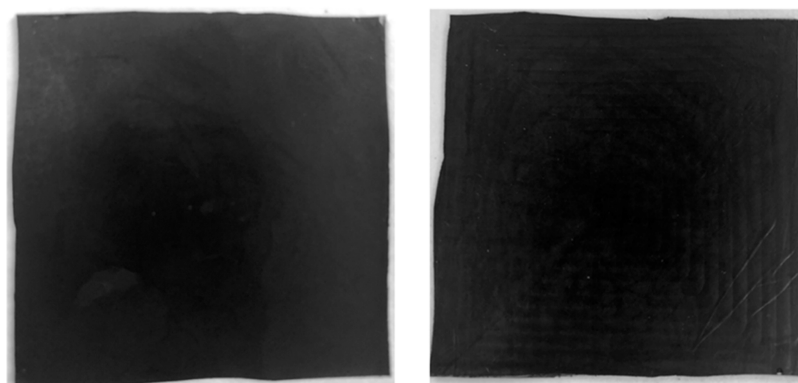
Figure 4. Front and back view of vitrimers after troubleshooting.

During the curing process, the carboxylic acid groups from OxL-COOH react with the epoxy groups from PEG-epoxy, in the presence of $Zn(acac)_2$.

During vitrimer formation, bubble formation was one of the main challenges encountered, as shown in Figure 3. Bubble formation in the film is linked to the nonhomogeneous mixing of OxL-COOH in ethanol and the leftover traces of solvent in the film before curing at the reaction temperatures. To address this, traces of insoluble impurities from the OxL-COOH/ethanol solution were initially separated from ethanol. In the soluble fraction, OxL-COOH was completely dissolved in the solvent, which is crucial for uniform film formation. Furthermore, the addition of $Zn(acac)_2$ and PEG-epoxy to this fraction allows for a completely homogeneous solution. Typically, ethanol is allowed to evaporate at 25 °C for 1 h, followed by at 80 °C for 1 h.[1,30] However, the OxL-COOH/PEG-epoxy systems possessed traces of ethanol before its transfer to the PTFE mold. As a result, nonuniform and brittle films were formed, limiting the overall tensile properties of the polymer. To address this, experiments were conducted by heating at 25 °C for 1 h followed by heating for 1, 2, 3, and 4 h at 80, 90, 100, and 110 °C, respectively. The optimum conditions for uniform film formation were observed at 110 °C with a heating duration of 4 h. At the optimized conditions, a homogeneous and uniform film was formed without any bubble formation, as shown in Figure 4.

Structural Characterization. *FTIR Analysis.* FTIR analysis was performed for untreated SKL, oxygen-treated (stage 1) L-COOH, and sequentially oxidized kraft lignin (stage 2) OxL-COOH samples. Figure 5 shows the broadening of peaks for $-C{=}O$ and $-OH$ groups at 1708 and $2500-3500$ cm^{-1},
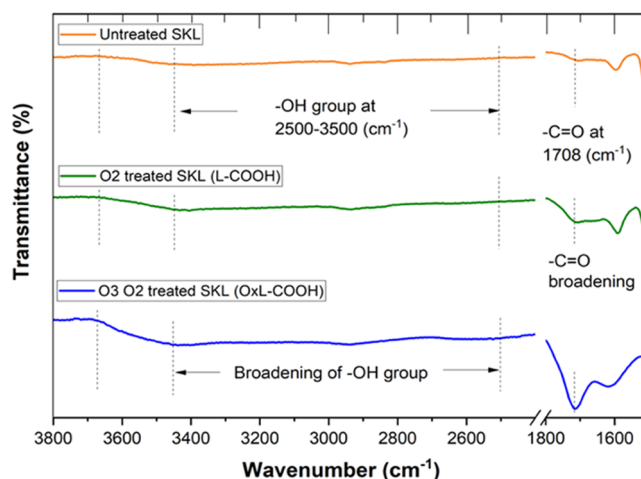
Figure 5. Comparative FTIR spectra of untreated SKL, oxygen-oxidized SKL (L-COOH), and oxygen- and ozone-treated SKL (OxL-COOH). The term O2 represents O_2 for oxygen oxidation and the term O3 O2 represents sequential oxidation using O_2 followed by O_3 oxidation.

respectively, as the severity of oxidation increased from oxygen to ozone. The $-OH$ group belongs to the $-COOH$ group. Therefore, from the qualitative analysis, it was confirmed that sequential oxidation enhances the carboxyl group formation in lignin. Thus, the improvement in carboxyl content was confirmed qualitatively using FTIR and quantitatively using ^{31}P NMR spectroscopy and conductometric titrations.

Table 2 shows the different stoichiometric formulations of the OxL-COOH/PEG-epoxy systems. All systems had high

Table 2. Different Stoichiometric Formulations of OxL-COOH/PEG-Epoxy Systems

lignin content (% by wt)	stoichiometric ratio "R" (epoxy/carboxyl)	mass ratio "R" (epoxy/carboxyl)	FWHM of tan δ (°C)	T_{d5} (°C)
39.6	1.5	1:0.65	−15	270
43.1	1.3	1:0.76	−10	276
49.5	1.0	1:0.98	−8	260

lignin content (≤50 wt %) with varying "R" values, implying a high biomass content in the polymer films. Figure 6 shows the
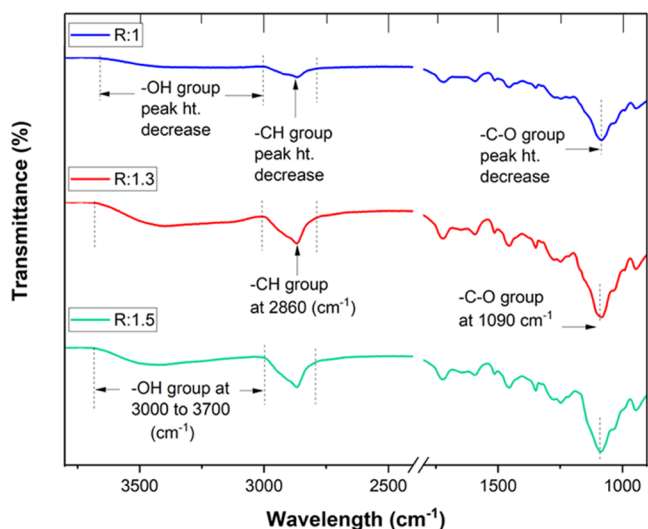
Figure 6. FTIR spectral changes of the cured OxL-COOH/PEG-epoxy system at different stoichiometric "R" values.

FTIR spectra of the cured PEG-epoxy/OxL-COOH samples with different "R" values. The peak intensity of epoxy groups from −C−O stretching (1090 cm^{-1}), −OH groups (3000−3700 cm^{-1}), and −C−H groups (2860 cm^{-1}) changed consistently with varying stoichiometric ratios. The increase in the "R" value from 1 to 1.5 increased the peak intensity of hydroxyl groups. As the "R" value approaches the stoichiometric value of R_t: 0.5, more complete curing is obtained; as a result, the peak intensity at 910 and 3400 cm^{-1} is reduced. However, as the "R" value increases, a high content of hydroxyl groups due to the ring opening of epoxy groups in PEG-epoxy occurs, which increases the peak intensity of the hydroxyl groups.

Dynamic Mechanical Properties. Dynamic mechanical analysis (DMA) was performed for all OxL-COOH/PEG-epoxy systems. Figure 7 shows the tensile modulus versus temperature of the cured OxL-COOH/PEG-epoxy systems. All curves exhibit a high storage modulus that defines the stiffness of the backbone structure and cross-link density. The storage modulus of OxL-COOH/PEG-epoxy increases as the lignin content increases, as lignin is much stiffer and possesses multiple reactive groups compared to PEG-epoxy. The full width at half-maximum (FWHM), which relates to the uniformity of the network, was also determined using DMA (Figure 8). The increase in lignin content also resulted in an increase in the full width at half-maximum due to the polydisperse nature of lignin. All OxL-COOH/PEG-epoxy systems showed a single glass transition based on the peak temperature of tan δ. The maximum storage modulus value of
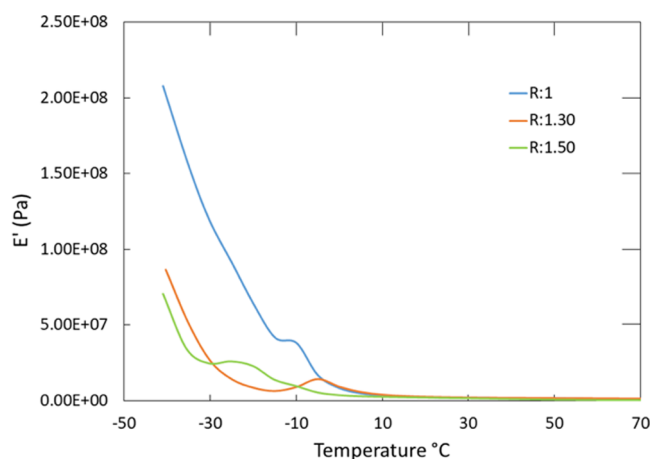
Figure 7. Storage modulus of OxL-COOH/PEG-epoxy films with different R values.
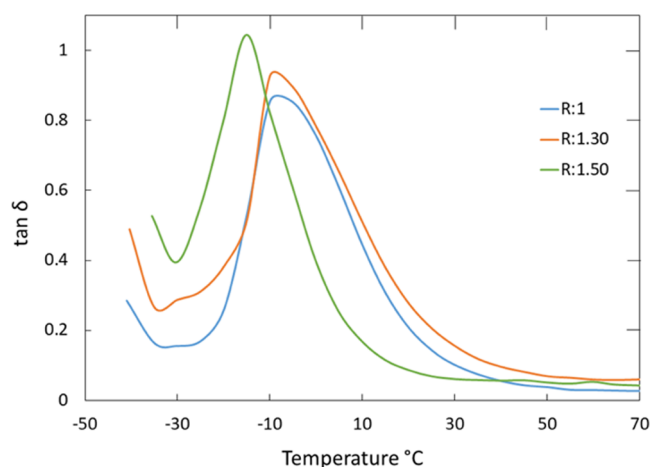
Figure 8. Tan δ of OxL-COOH/PEG-epoxy films with different R values.

2.08×10^8 Pa was obtained at the stoichiometric value of R:1. However, as the "R" value increased, the initial storage modulus values dropped to 8.7×10^7 and 7.06×10^7 Pa for R:1.30 and R:1.50, respectively.

Thermogravimetric Analysis. The thermogravimetric analysis and derivative thermogravimetric analysis study of poly(ethylene glycol) diglycidyl ether (PEGDE) with a molecular weight M_w of 500 g mol^{-1} has been reported in the literature.[51] Figure 9 shows that the 5% weight loss temperature (T_{d5}) of PEG-epoxy is below 200 °C. It was found that the PEG-epoxy thermal decomposition started at about 125 °C and was completely degraded at about 500 °C. In the DTG curve, the temperature at which the maximum weight loss rate occurred (T_{max}) was ~300 °C.

Thermogravimetric analysis (TGA) was performed on untreated SKL and all PEG-epoxy/OxL-COOH systems. The data obtained from TGA are crucial for understanding the thermal processing and stability of the vitrimers. The untreated SKL sample showed a 5% weight loss temperature at 112 °C (Figure S4). The weight loss at this temperature is the result of the expulsion of water molecules from the surface of SKL. In contrast, all PEG-epoxy/OxL-COOH systems showed a similar 5% weight loss temperature of ~270 °C, which was markedly higher than that of the untreated SKL, as shown in Figure 10. A higher residue content was obtained as the lignin content
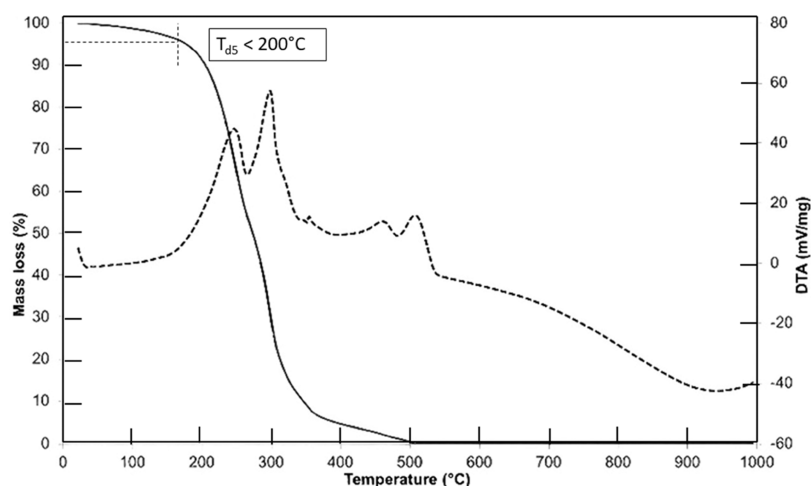
Figure 9. Thermogravimetric analysis (TGA) and derivative thermogravimetric analysis (DTG) study of PEG-epoxy (DTA* in the graph corresponds to DTG analysis). Reprinted with permission from ref 51. Copyright 2020 MDPI. Creative Commons Attribution (CC BY) license (http://creativecommons.org/licenses/by/4.0/).
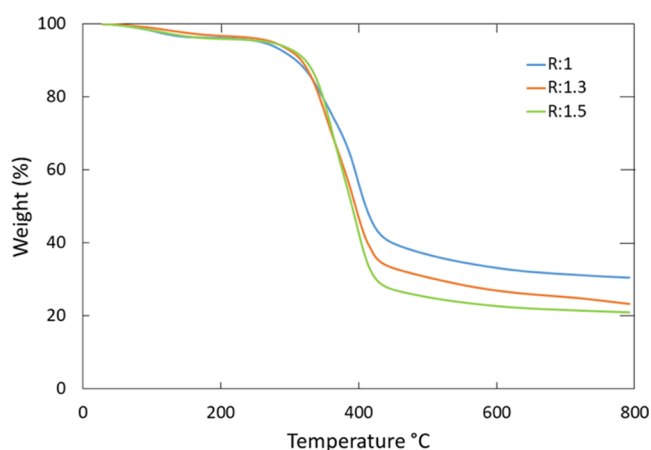
Figure 10. Thermogravimetric analysis (TGA) of OxL-COOH/PEG-epoxy films with different *R* values.
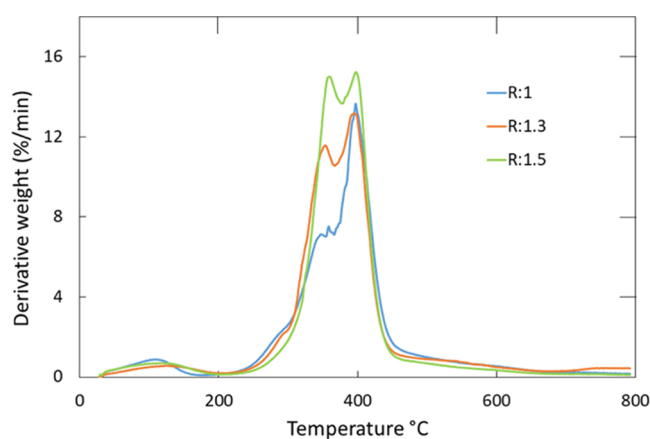
Figure 11. Derivative thermogravimetric analysis (DTG) of OxL-COOH/PEG-epoxy films with different *R* values.

increased due to the higher thermal stability of the sample and higher aromatic ring content. The temperature at which the maximum weight loss rate occurred for the OxL-COOH/PEG-epoxy systems was around 397 °C (Figure 11). These results indicate adequate thermostability of the samples for relaxation tests at elevated temperatures.

Stress Relaxation. Conventional thermosets are difficult to stress relax due to the permanent covalent bonds in the cross-linked structure. Figure 12 shows the stress relaxation behavior of a conventional epoxy thermoset at different temperatures ranging from 80 to 200 °C reported in the literature.[52] This epoxy thermoset was prepared by the diglycidyl ether of bisphenol A (DGEBA), glutaric anhydride, and zinc acetylacetonate $Zn(acac)_2$. From the graph, it is evident that conventional epoxy-based thermosets are difficult to stress relax at lower temperatures. However, due to the nature of associative bond exchange chemistry, vitrimers can undergo stress relaxation.

In this type of covalent adaptable network, bonds are only broken when a new covalent bond is formed resulting in a fixed cross-link density and making the network permanent as well as dynamic. Therefore, a stress relaxation test can provide direct evidence of transesterification exchange reactions
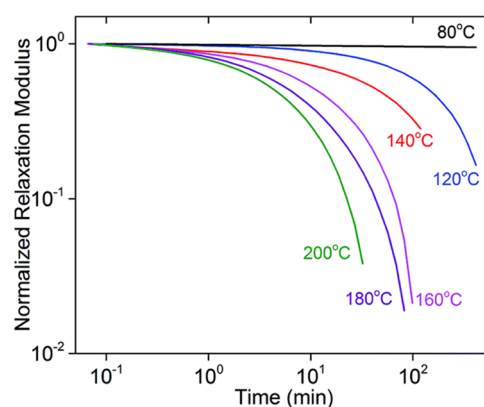
Figure 12. Stress relaxation behavior of the epoxy thermoset prepared from DGEBA, glutaric anhydride, and $Zn(acac)_2$ at different temperatures ranging from 80 to 200 °C. Reprinted with permission from ref 52. Copyright 2014 Royal Society of Chemistry.

(TERs). Figure 13 shows the stress relaxation modulus of OxL-COOH/PEG-epoxy films as a function of time at room temperature. All samples exhibited stress relaxation. The sample with *R*:1 demonstrated the fastest relaxation rate due to efficient TERs with ester bonds. However, the increase in
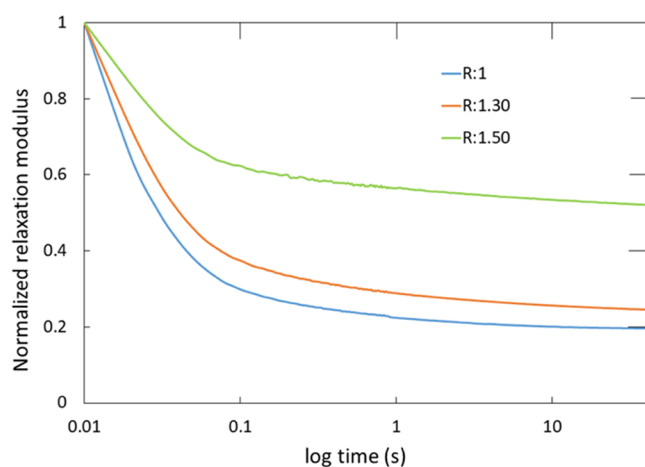
Figure 13. Stress relaxation curves of OxL-COOH/PEG-epoxy films with different *R* values.

Figure 14. Swelling of OxL-COOH/PEG-epoxy with *R*:1 in NaOH solutions with different concentrations (0.01, 0.05, 0.1, and 0.2 M).

Figure 15. Swelling of OxL-COOH/PEG-epoxy with *R*:1 in a 0.1 M NaOH solution at different time intervals (0, 5, 10, 15, 20, 30, and 60 min).

the stoichiometric value led to a slower relaxation rate due to the presence of unreacted hydroxyl groups from the ring opening of epoxy groups.

Swelling Study. In response to temperature and solvents, thermoplastic polymers completely dissolve and behave like a viscoelastic liquid when heated above a certain temperature, whereas thermosetting polymers can only swell and, even at higher temperatures, become softer but do not flow, and only a fraction of the polymer material dissolves. Vitrimer polymers represent a third category of organic polymers that behave like a viscoelastic liquid when heated and resist dissolution in good solvents.[53] OxL-COOH shows excellent solubility in aqueous NaOH solutions due to the nature of the lignin macromolecule. The deprotonation of lignin molecules is more favorable when the pH is above the pK_a value of 10.6, thereby contributing to its solubility in aqueous NaOH solutions.[24,54] At a given pH that is below the pK_a of lignin, the protonated form is favored in the equilibrium between protonated and deprotonated forms.

In contrast, at lower pH values, there is less dissociation of the charged phenolic OH groups in lignin. Also, the phenol and carboxyl groups from lignin can transform into sodium phenolate and sodium carboxylate ions in aqueous NaOH solutions, thereby contributing to the solubility. Therefore, aqueous NaOH solutions represent an excellent medium to test the swelling nature of the OxL-COOH/PEG-epoxy system. Figure 14 shows the swelling OxL-COOH/PEG-epoxy with *R*: 1 in NaOH solutions with concentrations of 0.01, 0.05, 0.1, and 0.2 M with swelling time fixed at 10 min. The swelling trend showed a slow increase from 0.01 to 0.05 M followed by a rapid increase to 0.2 M. As the concentration changed from 0.01 to 0.2 M, the swelling increased from 13.5 to 44.9%, which shows significant improvement in the swelling of the vitrimer. To understand the effect of time on the swelling of OxL-COOH/PEG-epoxy systems, the sample was monitored at continuous time intervals starting from 0 up to 60 min (Figure 15) in a 0.1 M NaOH solution. The swelling increased rapidly to 40.1% in the first 15 min, after which the swelling continuously increased but at a slower rate. The lines between the points in plots shown in Figures 14 and 15 are used as a guide to the eye. The noteworthy swelling of the vitrimer in an alkaline solution signifies the occurrence of transesterification exchange reactions of the OxL-COOH/PEG-epoxy systems.
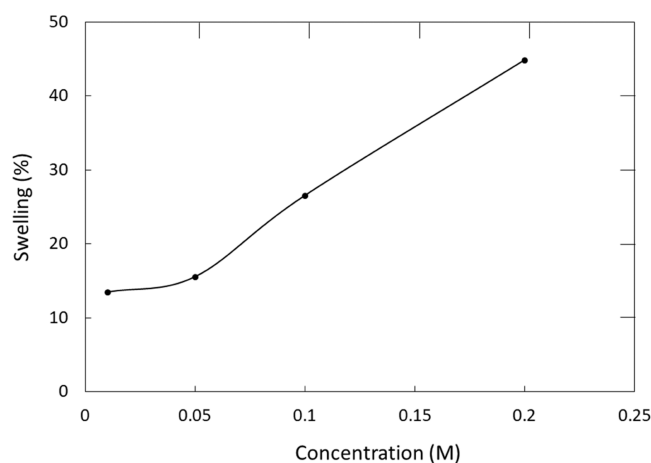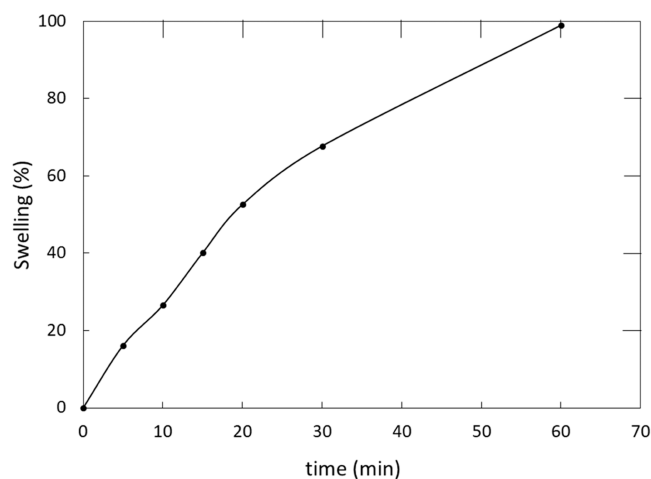
Self-Healing. In addition to swelling, self-healing constitutes an important feature of vitrimers due to the dynamic transesterification exchange reactions. The detailed image description of self-healing is shown in Figures S7−S15. The self-healing (%) of these samples versus time duration (min) is shown in Figure 16.

The precise molecular mechanism governing the microscale self-healing is under current investigation, and the sample viscosity is close to 10^7 Pa·s at room temperature, which is too large for gravity-driven flow on these time scales.[55] Samples *R*:1 and *R*:1.3 showed a rapid healing response facilitated by the dynamic bonds at elevated temperatures. The use of heat treatment for self-healing the films in the absence of pressure and solvent demonstrates a convenient and promising method for repair in coating applications. At low temperatures, the cross-linked structure is generally frozen; however, as the temperature is increased, dynamic transesterification is promoted, and self-healing is triggered. For the sample with *R*:1, the average crack width of 17.5 μm changed to 11.87 μm in the first 15 min and to 8.03 μm in the next 15 min, as shown in Figure 17. Overall, the crack width of this sample healed to about 54.1% in the first 30 min. In contrast, in the sample with *R*:1.3, the average crack width of 10.33 μm changed rapidly to
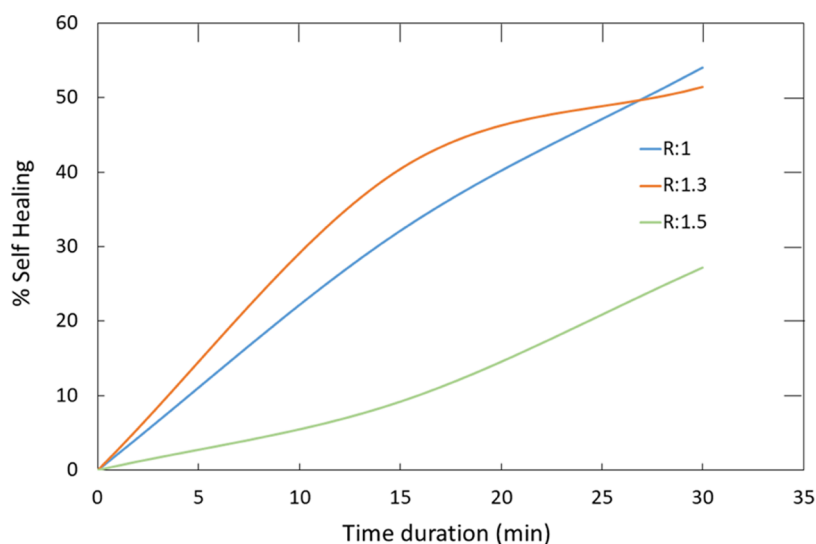
Figure 16. Rate of self-healing in different OxL-COOH/PEG-epoxy samples.

| R:1 sample after crack | R:1 sample after 15 min curing | R:1 sample after 30 min curing |
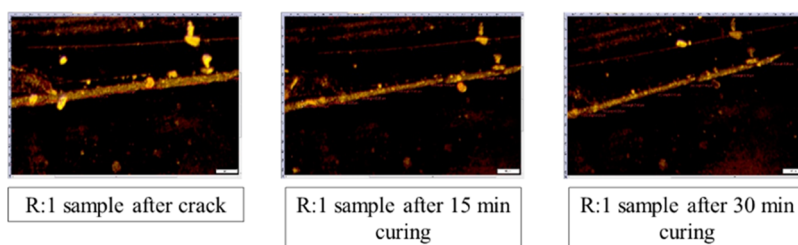
Figure 17. Self-healing for the R:1 sample after crack, after 15 min curing, and after 30 min curing.

6.15 μm in the first 15 min and slowly to 5.01 μm in the next 15 min. At R:1.5, the initial crack width of 8.37 μm changed slightly to 7.6 μm in the first 15 min and to 6.09 μm. Overall, this sample represented the slowest repairability compared with R:1.3 and R:1. As confirmed with other studies, the sample with R:1 represented efficient transesterification exchange reactions due to the nature of self-healing observed in this sample.

CONCLUSIONS

The objective of this work was to maximize lignin utilization to produce diverse value-added products with a focus on integration in existing pulp and paper industrial processes. Based on the results obtained, oxidation of SKL represents a new approach for production of vanillin and vanillic acid from oxygen oxidation followed by lignin-containing vitrimers from sequential oxidation, which diversify the value-added product profile from lignin. The modification of SKL using ozone represents a lignin source with high carboxyl content, which is crucial for vitrimer formation with PEG-epoxy. All OxL-COOH/PEG-epoxy systems possessed a high lignin content (>48 wt %). All systems showed thermal stability, fast relaxation, and self-healing due to the presence of bond-exchangeable cross-linked networks. In aqueous NaOH solutions, the lignin-containing vitrimer did not dissolve and exhibited noteworthy swelling properties, which is a key indicator of the dynamic transesterification in the cured network. Overall, this study represents a novel and integrated process for the valorization of kraft lignin into value-added products.

ASSOCIATED CONTENT

Supporting Information

The Supporting Information is available free of charge at https://pubs.acs.org/doi/10.1021/acsomega.2c06445.

^{31}P NMR spectra of untreated and oxygen-treated softwood kraft lignin; effect of ozone on the carboxyl content of kraft lignin; thermogravimetric analysis (TGA) and derivative thermogravimetric analysis (DTG) of untreated kraft lignin; swelling ability of the vitrimer system; and self-healing ability of vitrimers at different stoichiometric ratios (PDF)

AUTHOR INFORMATION

Corresponding Author

Zhihua Jiang − *Alabama Center for Paper and Bioresource Engineering (AC-PABE), Department of Chemical Engineering, Auburn University, Auburn, Alabama 36849, United States;* orcid.org/0000-0001-5020-7745; Phone: (+1) 334-844-7829; Email: zzj0012@auburn.edu

Authors

Ajinkya More − *Alabama Center for Paper and Bioresource Engineering (AC-PABE), Department of Chemical Engineering, Auburn University, Auburn, Alabama 36849, United States;* orcid.org/0000-0002-7312-6216

Thomas Elder − *United States Department of Agriculture, U.S. Forest Service, Auburn, Alabama 36849, United States;* orcid.org/0000-0003-3909-2152

Nicolò Pajer − *Department of Molecular Sciences and Nanosystems, Ca' Foscari University of Venice, Venezia, Mestre 30172, Italy*

Dimitris S. Argyropoulos − *Department of Forest Biomaterials, NC State University, Raleigh, North Carolina 27695-8005, United States*

Complete contact information is available at:
https://pubs.acs.org/10.1021/acsomega.2c06445

Notes

The authors declare no competing financial interest.

◼ REFERENCES

(1) Zhang, S.; Liu, T.; Hao, C.; Wang, L.; Han, J.; Liu, H.; Zhang, J. Preparation of a lignin-based vitrimer material and its potential use for recoverable adhesives. *Green Chem.* **2018**, *20*, 2995−3000.

(2) Post, W.; Susa, A.; Blaauw, R.; Molenveld, K.; Knoop, R. J. A review on the potential and limitations of recyclable thermosets for structural applications. *Polym. Rev.* **2020**, *60*, 359−388.

(3) Montarnal, D.; Capelot, M.; Tournilhac, F.; Leibler, L. Silica-like malleable materials from permanent organic networks. *Science* **2011**, *334*, 965−968.

(4) Kloxin, C. J.; Scott, T. F.; Adzima, B. J.; Bowman, C. N. Covalent adaptable networks (CANs): a unique paradigm in cross-linked polymers. *Macromolecules* **2010**, *43*, 2643−2653.

(5) Denissen, W.; Winne, J. M.; Du Prez, F. E. Vitrimers: permanent organic networks with glass-like fluidity. *Chem. Sci.* **2016**, *7*, 30−38.

(6) Liu, T.; Guo, X.; Liu, W.; Hao, C.; Wang, L.; Hiscox, W. C.; Liu, C.; Jin, C.; Xin, J.; Zhang, J. Selective cleavage of ester linkages of anhydride-cured epoxy using a benign method and reuse of the decomposed polymer in new epoxy preparation. *Green Chem.* **2017**, *19*, 4364−4372.

(7) Liu, T.; Hao, C.; Wang, L.; Li, Y.; Liu, W.; Xin, J.; Zhang, J. Eugenol-derived biobased epoxy: shape memory, repairing, and recyclability. *Macromolecules* **2017**, *50*, 8588−8597.

(8) Altuna, F. I.; Pettarin, V.; Williams, R. J. Self-healable polymer networks based on the cross-linking of epoxidized soybean oil by an aqueous citric acid solution. *Green Chem.* **2013**, *15*, 3360−3366.

(9) Ma, Z.; Wang, Y.; Zhu, J.; Yu, J.; Hu, Z. Bio-based epoxy vitrimers: Reprocessibility, controllable shape memory, and degradability. *Polym. Chem.* **2017**, *55*, 1790−1799.

(10) Boerjan, W.; Ralph, J.; Baucher, M. Lignin biosynthesis. *Annu. Rev. Plant Biol.* **2003**, *54*, 519−546.

(11) Cazacu, G.; Pascu, M. C.; Profire, L.; Kowarski, A.; Mihaes, M.; Vasile, C. Lignin role in a complex polyolefin blend. *Ind. Crops Prod.* **2004**, *20*, 261−273.

(12) More, A.; Elder, T.; Jiang, Z. A review of lignin hydrogen peroxide oxidation chemistry with emphasis on aromatic aldehydes and acids. *Holzforschung* **2021**, *75*, 806−823.

(13) Pinto, P. C. R.; da Silva, E. A. B.; Rodrigues, A. E. *Lignin as Source of Fine Chemicals: Vanillin and Syringaldehyde: Biomass Conversion*; Springer, 2012; pp 381−420.

(14) Bajwa, D.; Pourhashem, G.; Ullah, A.; Bajwa, S. A concise review of current lignin production, applications, products and their environmental impact. *Ind. Crops Prod.* **2019**, *139*, No. 111526.

(15) Hu, T. Q. *Chemical Modification, Properties, and Usage of Lignin*; Springer, 2002.

(16) Schorr, D.; Diouf, P. N.; Stevanovic, T. Evaluation of industrial lignins for biocomposites production. *Ind. Crops Prod.* **2014**, *52*, 65−73.

(17) Chatel, G.; Rogers, R. D. Oxidation of lignin using ionic liquids: An innovative strategy to produce renewable chemicals. *ACS Sustainable Chem. Eng.* **2014**, *2*, 322−339.

(18) Das, A.; Rahimi, A.; Ulbrich, A.; Alherech, M.; Motagamwala, A. H.; Bhalla, A.; da Costa Sousa, L.; Balan, V.; Dumesic, J. A.; Hegg, E. L.; et al. Lignin conversion to low-molecular-weight aromatics via an aerobic oxidation-hydrolysis sequence: comparison of different lignin sources. *ACS Sustainable Chem. Eng.* **2018**, *6*, 3367−3374.

(19) Abdelaziz, O. Y.; Ravi, K.; Mittermeier, F.; Meier, S.; Riisager, A.; Lidén, G.; Hulteberg, C. P. Oxidative depolymerization of kraft lignin for microbial conversion. *ACS Sustainable Chem. Eng.* **2019**, *7*, 11640−11652.

(20) Tarabanko, V. E.; Tarabanko, N. Catalytic oxidation of lignins into the aromatic aldehydes: general process trends and development prospects. *Int. J. Mol. Sci.* **2017**, *18*, 2421.

(21) Bezerra, D. P.; Soares, A. K. N.; de Sousa, D. P. Overview of the role of vanillin on redox status and cancer development. *Oxid. Med. Cell. Longevity* **2016**, *2016*, No. 9734816.

(22) Choo, J.; Rukayadi, Y.; Hwang, J. K. Inhibition of bacterial quorum sensing by vanilla extract. *Lett. Appl. Microbiol.* **2006**, *6*, 637−641.

(23) Calixto-Campos, C. S.; Carvalho, T. T.; Hohmann, M. S.; Pinho-Ribeiro, F. A.; Fattori, V.; Manchope, M. F.; Zarpelon, A. C.; Baracat, M. M.; Georgetti, S. R.; Casagrande, R.; Verri, W. A. Vanillic acid inhibits inflammatory pain by inhibiting neutrophil recruitment, oxidative stress, cytokine production, and NFκB activation in mice. *J. Nat. Prod.* **2015**, *78*, 1799−1808.

(24) Kouisni, L.; Paleologou, M. Method for Separating Lignin From Black Liquor. U.S. Patent US8486224B2, 2014.

(25) Kouisni, L.; Holt-Hindle, P.; Maki, K.; Paleologou, M. The lignoforce system: a new process for the production of high-quality lignin from black liquor. *J. Sci. Technol. Prod. Process.* **2012**, *2*, 6−10.

(26) Wells, K.; Pors, D.; Foan, J.; Maki, K.; Kouisni, L.; Paleologou, M. In *CO₂ Impacts of Commercial Scale Lignin Extraction at Hinton Pulp Using the LignoForce Process & Lignin Substitution into Petroleum-Based Products*, PACWEST Conference, 2015; pp 10−13.

(27) Kouisni, L.; Gagne, A.; Maki, K.; Holt-Hindle, P.; Paleologou, M. LignoForce system for the recovery of lignin from black liquor: feedstock options, odor profile, and product characterization. *ACS Sustainable Chem. Eng.* **2016**, *4*, 5152−5159.

(28) More, A.; Elder, T. J.; Jiang, Z. Towards a new understanding of the retro-aldol reaction for oxidative conversion of lignin to aromatic aldehydes and acids. *Int. J. Biol. Macromol.* **2021**, *183*, 1505−1513.

(29) Han, J.; Liu, T.; Hao, C.; Zhang, S.; Guo, B.; Zhang, J. A catalyst-free epoxy vitrimer system based on multifunctional hyperbranched polymer. *Macromolecules* **2018**, *51*, 6789−6799.

(30) Hao, C.; Liu, T.; Zhang, S.; Brown, L.; Li, R.; Xin, J.; Zhong, T.; Jiang, L.; Zhang, J. A High-Lignin-Content, Removable, and Glycol-Assisted Repairable Coating Based on Dynamic Covalent Bonds. *ChemSusChem* **2019**, *12*, 1049−1058.

(31) Jin, X.; Liu, X.; Li, X.; Du, L.; Su, L.; Ma, Y.; Ren, S. High lignin, light-driven shape memory polymers with excellent mechanical performance. *Int. J. Biol. Macromol.* **2022**, *219*, 44−52.

(32) Du, L.; Jin, X.; Qian, G.; Yang, W.; Su, L.; Ma, Y.; Ren, S.; Li, S. Lignin-based vitrimer for circulation in plastics, coatings, and adhesives with tough mechanical properties, catalyst-free and good chemical solvent resistance. *Ind. Crops Prod.* **2022**, *187*, No. 115439.

(33) Asgari, F.; Argyropoulos, D. S. Fundamentals of oxygen delignification. Part II. Functional group formation/elimination in residual kraft lignin. *Can. J. Chem.* **1998**, *76*, 1606−1615.

(34) Gierer, J.; Imsgard, F. The reactions of lignins with oxygen and hydrogen peroxide in alkaline media. *Sven. Papperstidn.* **1997**, *80*, 510−518.

(35) Chang, H.; Gratzl, J. Ring Cleavage Reactions of Lignin Models with Oxygen and Alkali. In *Chemistry of Delignification with Oxygen, Ozone and Peroxides*; Singh, R. P.; Nakano, J.; Gratzl, Eds.; Uni Publishers Co. Ltd.: Tokyo, 1980; pp 151−163.

(36) Fernandes, M. R.; Huang, X.; Abbenhuis, H. C.; Hensen, E. J. Lignin oxidation with an organic peroxide and subsequent aromatic ring opening. *Int. J. Biol. Macromol.* **2019**, *123*, 1044−1051.

(37) Liu, T.; Zhao, B.; Zhang, J. Recent development of repairable, malleable and recyclable thermosetting polymers through dynamic transesterification. *Polymer* **2020**, *194*, No. 122392.

(38) Musl, O.; Holzlechner, M.; Winklehner, S.; Gübitz, G.; Potthast, A.; Rosenau, T.; Böhmdorfer, S. Changing the Molecular Structure of Kraft Lignins—Ozone Treatment at Alkaline Conditions. *ACS Sustainable Chem. Eng.* **2019**, *7*, 15163−15172.

(39) Meng, X.; Crestini, C.; Ben, H.; Hao, N.; Pu, Y.; Ragauskas, A. J.; Argyropoulos, D. S. Determination of hydroxyl groups in biorefinery resources via quantitative ^{31}P NMR spectroscopy. *Nat. Protoc.* **2019**, *14*, 2627−2647.

(40) Katz, S.; Beatson, R. P. The determination of strong and weak acidic groups in sulfite pulps. *Sven. Papperstidn.* **1984**, *87*, 48−53.

(41) Jiang, Z.Advances and Applications of Quantitative ^{31}P NMR for the Structural Elucidation of Lignin, Ph.D. Thesis, McGill University: Canada, 1997.

(42) Gellerstedt, G.; Lindfors, E. L. Structural changes in lignin during kraft pulping. *Holzforschung* **1984**, *38*, 151−158.

(43) Ma, R.; Xu, Y.; Zhang, X. Catalytic oxidation of biorefinery lignin to value-added chemicals to support sustainable biofuel production. *ChemSusChem* **2015**, *8*, 24−51.

(44) Gellerstedt, G.; Gustafsson, K.; Lindfors, E. L. Structural changes in lignin during oxygen bleaching. *Nord. Pulp Pap. Res. J.* **1986**, *1*, 14−17.

(45) Sun, Y.; Argyropoulos, D. S. Fundamentals of high-pressure oxygen and low-pressure oxygen-peroxide (EOP) delignification of softwood and hardwood kraft pulps: a comparison. *J. Pulp Pap. Sci.* **1995**, *21*, J185−J190.

(46) Denissen, W.; Winne, J. M.; Du Prez, F. E. Vitrimers: permanent organic networks with glass like fluidity. *Chem. Sci.* **2016**, *7*, 30−38.

(47) Moreno, A.; Morsali, M.; Sipponen, M. H. Catalyst-free synthesis of lignin vitrimers with tunable mechanical properties: Circular polymers and recoverable adhesives. *ACS Appl. Mater. Interfaces* **2021**, *13*, 57952−57961.

(48) Geng, H.; Wang, Y.; Yu, Q.; Gu, S.; Zhou, Y.; Xu, W.; Zhang, X.; Ye, D. Vanillin-based polyschiff vitrimers: reprocessability and chemical recyclability. *ACS Sustainable Chem. Eng.* **2018**, *6*, 15463−15470.

(49) Xue, B.; Tang, R.; Xue, D.; Guan, Y.; Sun, Y.; Zhao, W.; Tan, J.; Li, X. Sustainable alternative for bisphenol A epoxy resin high-performance and recyclable lignin-based epoxy vitrimers. *Ind. Crops Prod.* **2021**, *168*, No. 113583.

(50) Bass, G. F.; Epps, T. H., III Recent developments towards performance-enhancing lignin-based polymers. *Polym. Chem.* **2021**, *12*, 4130−4158.

(51) Mallard, I.; Landy, D.; Fourmentin, S. Evaluation of polyethylene glycol crosslinked β-CD polymers for the removal of methylene blue. *Appl. Sci.* **2020**, *10*, 4679.

(52) Yu, K.; Taynton, P.; Zhang, W.; Dunn, M. L.; Qi, H. J. Influence of stoichiometry on the glass transition and bond exchange reactions in epoxy thermoset polymers. *RSC Adv.* **2014**, *4*, 48682−48690.

(53) Winne, J. M.; Leibler, L.; Du Prez, F. E. Dynamic covalent chemistry in polymer networks: A mechanistic perspective. *Polym. Chem.* **2019**, *10*, 6091−6108.

(54) Zhu, W.; Theliander, H. Precipitation of lignin from softwood black liquor: an investigation of the equilibrium and molecular properties of lignin. *BioResources* **2014**, *10*, 1696−1714.

(55) Porath, L. E.; Evans, C. M. Importance of broad temperature windows and multiple rheological approaches for probing viscoelasticity and entropic elasticity in vitrimers. *Macromolecules* **2021**, *54*, 4782−4791.